BENIN JOURNAL OF PHYSICAL SCIENCES
BJPS Vol. 2(2), December, pg. 47-59 (2025)
ISSN 3043-6931(Print)
3043-694X(Online)
www.bjps.org.ng

Performance of a Horizontal Well Subject to Simultaneous Single Edge Water and Bottom Water Drive Mechanisms

A. M. MADAKI*,[1] and E. S. ADEWOLE[2]

[1]*Department of Petroleum Engineering, Federal University of Petroleum Resources Effurun, Delta State, Nigeria*
[2]*Department of Petroleum Engineering, University of Benin, Benin City, Nigeria*

Received: 16/09/2025 ***Accepted:*** 22/11/2025

Abstract

When a reservoir is bounded by one or more constant pressure boundaries, such as aquifer or gas cap, the main expectation of the production engineer is to delay the arrival of either water or gas into the well completed in the reservoir to optimize oil production. To achieve this expectation, it is important to understand fluid flow pattern through the reservoir system when oil is produced through the well. For a horizontal well, understanding the strategies to achieve optimum oil production in a reservoir subject to an edge water and bottom water acting simultaneously to provide drive energy in the reservoir poses challenges due to the complexity in well flow periods, aquifer activity and reservoir heterogeneity. In this paper, real time oil flow transient pressure model using dimensionless pressures and dimensionless pressure derivatives was developed using superposition principle and image method to investigate performance of a horizontal well subject simultaneously to single edge water and bottom water drive mechanisms. The model was tested to evaluate the horizontal well response to oil production transient flow for different well designs, reservoir anisotropy and well completions. Results obtained show three (3) images of the object well from inclination of single edge water and bottom water boundaries. Horizontal well productivity increases for slimmer wellbores and shorter wells, for a given well completion. Results further revealed that, locating the well farther away from the constant pressure boundaries leads to longer oil production than wells located closer to the boundaries. The time of influence of external reservoir boundaries increases with farther well location from the boundaries. Rapid oil production is achieved with stimulated wellbore and large anisotropy reservoirs than damaged wellbores and low anisotropy reservoirs. It is therefore concluded that. for optimum oil

*Corresponding author e-mail: aliyumadaki94@gmail.com

production from a horizontal well subject to single edge and bottom water drives is possible with slimmer well radius, short and stimulated wellbores and well location as far from the constant pressure boundaries as practicable.

Keywords: *Horizontal Well, Dimensionless Pressure, Dimensionless Pressure derivative, wellbore radius, Constant pressure boundaries*

1. INTRODUCTION

A horizontal well is a type of multi-directional wellbore that is drilled to an inclination of at least 80 degrees from vertical, extending horizontally through the target reservoir. This technique allows for significantly greater contact with the reservoir, improving oil recovery compared to traditional vertical wells, especially in thin layered or fractured formations. The well is initially drilled vertically to reach the target reservoir, then steered and curved to horizontal direction and continue to drilled horizontally through the pay zone maximizing the length of the reservoir exposed to the wellbore.

Water drive reservoir is an oil or gas reservoir connected to a large, active aquifer that provides natural pressure support mechanism. As hydrocarbons are extracted, the aquifer water expands and moves in to the reservoir, displacing the oil or gas towards the production wells. For the reservoir with bottom water drive, the aquifer is directly beneath the oil zone, as oil is produced the water moves vertically upward to occupy the space. While for edge water drive the aquifer is located on the flanks or edges of the hydrocarbon reservoir. The water moves laterally in to the oil zone, displacing the oil horizontally Dake (1978).

Nzomo et al. (2022) studied the performance of a horizontal well in a bounded anisotropic reservoir and revealed that reservoir anisotropy can be approximated during the infinite-acting flow at early times when other parameters are known. Also, Nzomo et al. (2023) worked on performance of a horizontal well in a bounded anisotropic reservoir and discovered that an increase in dimensionless well length decreases pressure response during the infinite-acting flow at early times and during transition flows at middle time but increases the pressure response during the pseudosteady state flow at late times. Olokor and Adewole (2024) discovered that, at late flow dimensionless time, dimensionless pressure gradients of 2.3026 $\propto/L_D$ per cycle characterize horizontal well in a pair of sealing boundaries inclined at 90^0. Agho (2022) indicates that dimensionless pressure rises as reservoir pay thickness increases, delaying steady-state conditions. Furthermore, distance from the constant pressure boundary, well length, and pay thickness are the most important factors in determining external fluid invasion in the wellbore. Oloro and Adewole (2019) discovered ten models for pressure distribution of a horizontal well under different boundary variation. Also, Oloro and Adewole (2020) discovered that wellbore pressure losses during production

in horizontal well increase conning propensity at late period thus rendering some part of the horizontal well unproductive. Ogunfeyimi and Adewole(2025) worked on productivity performance of a horizontal well in an oil reservoir bounded by bottom water and a sealing boundary inclined at 45^{o}.They provide a practical guidance for well placement, stimulation and design strategies to improve horizontal well productivity, when the well is completed within a pair of reservoirs mixed external boundaries.

Etuwe and Adewole (2025) studied the effects of horizontal well length on the pressure of a reservoir subject to double edge and bottom water drives. Their result shows that infinite acting period and the time of onset of late time flow with respect to pressure and pressure derivative, are mathematically inversely related to well length of a horizontal well. Orene and Adewole (2020) discovered that dimensionless lateral extent has no direct effect on dimensionless pressure and dimensionless pressure derivative for very short well lengths, Dimensionless pressure increases with reservoir pay thickness and delay the time for steady state conditions.. Superposition principle has been used by petroleum engineers to solve complex problems for many decades. The superposition principle states that the response of a given system caused by two or more stimuli is the sum of the responses of each individual stimulus Dunsmuir and Stewart (1989).

The goal of this study is to develop a mathematical model to study the performance of a horizontal well positioned between two constant pressure boundaries (an edge and bottom water) inclined at right angle in an anisotropic reservoir. The pressure response is simulated by analytical models that use the superposition principle and the method of images.

2. MATERIALS AND METHOD

Figure 1 is a schematic of a horizontal well drilled and completed within a pair of constant pressure boundaries (an edge and bottom water) of an oil reservoir inclined at right angle.

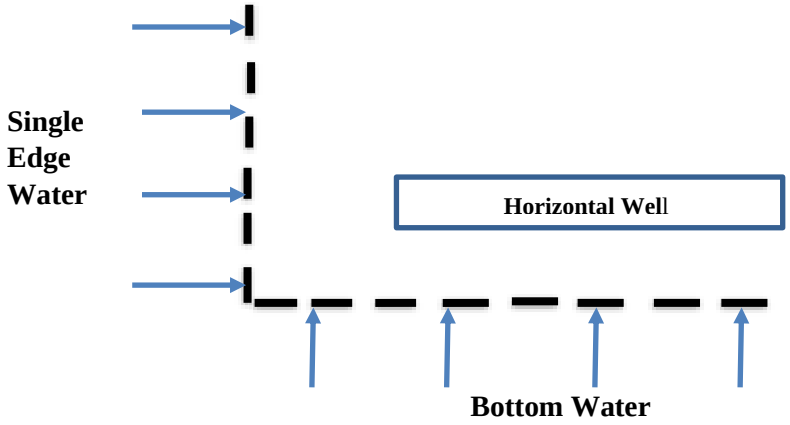

Figure 1: *Horizontal Well Completed within Oil Reservoir with Simultaneous Edge and Bottom Water Drives*

If the constant pressure boundaries are considered as plane mirrors, and the horizontal well is considered as an object well, Ow, placed at a distance d from the boundary then, the images of the wells are produced as illustrated in Figure 2.

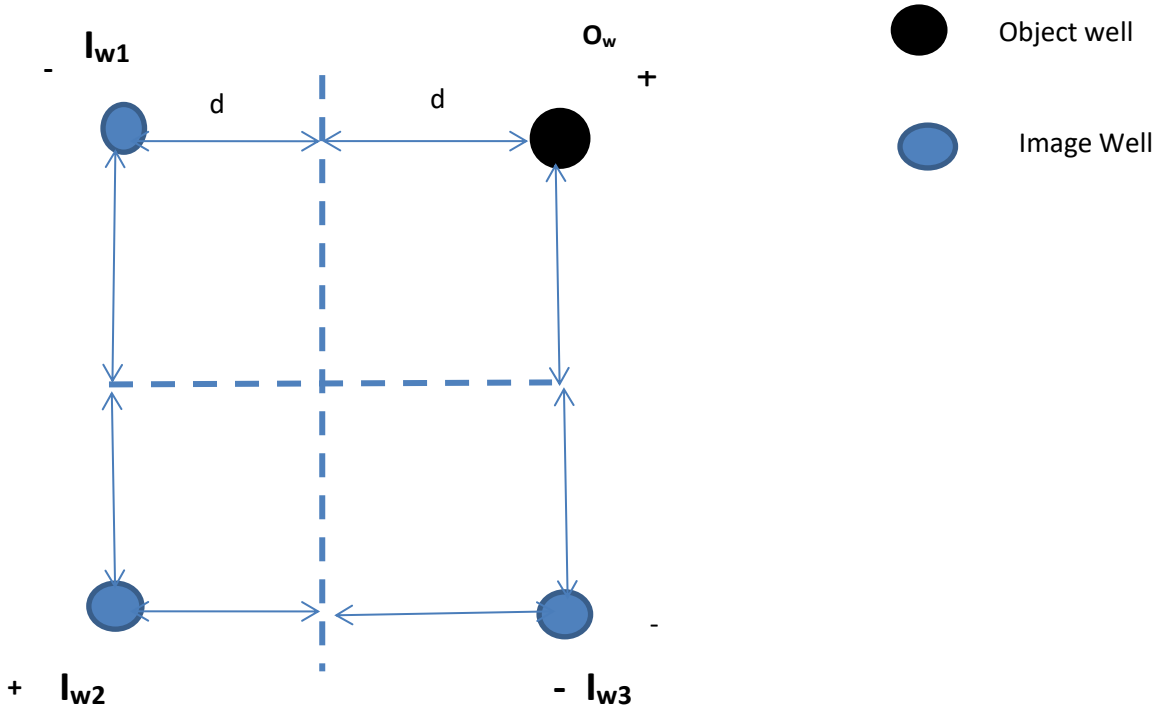

Figure 2: *Object Horizontal Well and Location of Images formed in an Oil Reservoir with Simultaneous Edge and Bottom Water Drives*

Three images were formed according to the plane mirror equation below.

$$n = \frac{360}{\theta} - 1 \qquad (1)$$

The distance between the object well and each image well can be measured by drawing or trigonometry.

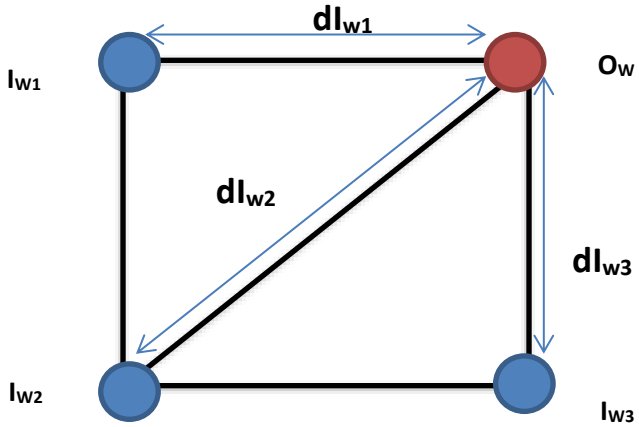

Figure 3: *Image wells and their respective distances from the Object well*

The Figure 3 depicts Image wells distances from the object horizontal well. The distance of the image well 2 (dI_{w2}) is obtained using trigonometry as shown in equation 2 below. While distance of image well 1, dI_{w1} is twice the distance of the object horizontal well from the first boundary and distance of image well 3 dI_{w3} is also twice the distance of the object horizontal well from the second boundary.

$$dI_{w2} = \sqrt{(dI_{w1})^2 + (dI_{w3})^2} \tag{2}$$

By superposition principle, the total dimensionless pressure drop in the object well is the summation of dimensionless pressure drop in the object well due to flow in the object well, dimensionless pressure drop in the object well due to flow in image well 1, dimensionless pressure drop in the object well due to flow in image well 2 and dimensionless pressure drop in the object well due to flow in image well 3. Mathematically, the total dimensionless pressure in the object well is

$$P_{DOw} = P_{DOw,ow} + P_{DOw,Iw1} + P_{DOw,Iw2} + P_{DOw,Iw3} \tag{3}$$

The superposition accounts for the reverberation effect of images on their sources as experienced in all physical and acoustic systems. For a horizontal well in isotropic reservoir, dimensionless pressure drop in the object well due to flow in the object well is given in Equation 4 (Nzomo et al (2022).

$$P_{DOw,Ow} = -\frac{\propto}{4L_D}\left[Ei\left(-\frac{r_{wD}^2}{4t_D/C_D}\right)\right] + s_{oW} \tag{4}$$

Following Equation 4, dimensionless pressure drop in the object well due to flow in image well i can be written as follows:

$$P_{DOw,Iwi} = \frac{\propto}{4L_D}\left[Ei\left(-\frac{(dI_{wi})^2}{4t_D}\right)\right] \tag{5}$$

The total dimensionless pressure drop in Equation 3 is therefore written as follows:

$$P_D = \frac{\propto}{4L_D}\left[\left\{-Ei\left(-\frac{r_{wD}^2}{4t_D/C_D}\right) + Ei\left(-\frac{(dI_{w1})^2}{4t_D}\right) - Ei\left(-\frac{(dI_{w2})^2}{4t_D}\right) + Ei\left(-\frac{(dI_{w3})^2}{4t_D}\right)\right\}\right] + S_{OW} \tag{6}$$

To account for reservoir anisotropy, Equation 8 becomes

$$P_D = \frac{\propto}{4L_D}\sqrt{\frac{k}{k_x}}\sqrt{\frac{k}{k_y}}\sqrt{\frac{k}{k_z}}\left[-Ei\left(-\frac{r_{wD}^2}{4t_D/C_D}\right) + Ei\left(-\frac{(dI_{w1})^2}{4t_D}\right) - Ei\left(-\frac{(dI_{w2})^2}{4t_D}\right) + Ei\left(-\frac{(dI_{w3})^2}{4t_D}\right)\right] + S_{OW} \quad (7)$$

Dimensionless pressure derivative is given as

$$P'_D = t_D\frac{\partial p_D}{\partial t_D} \quad (8)$$

Therefore, the dimensionless pressure derivative is derived for Equation (7) as:

$$P'_D = \frac{\propto}{4L_D}\sqrt{\frac{k}{k_x}}\sqrt{\frac{k}{k_y}}\sqrt{\frac{k}{k_z}}\left[exp\left(-\frac{r_{wD}^2}{4t_D/C_D}\right) - exp\left(-\frac{(dI_{w1})^2}{4t_D}\right) + exp\left(-\frac{(dI_{w2})^2}{4t_D}\right) - exp\left(-\frac{(dI_{w3})^2}{4t_D}\right)\right] \quad (9)$$

3. RESULT AND DISCUSSION

As observed from Figure 4 below, increase in dimensionless well radius result to decrease in dimensionless pressures. Also the dimensionless pressure P_D values increase with increase in dimensionless time t_D, from t_D = 0.001 to 100 and later maintain a stable value from t_D=1000 onward which signaled steady state flow, as the flow encountered the effect of constant pressure boundary. Figure 5.0 shows that the change in dimensionless well radius r_{wD} has no significant effect on P_D' as the curves for varying r_{wD} merged to form single curve , also changing r_{wD} values has no effect on breakthrough time as P_D' curve intersect t_D axes at t_D =1000 for all r_{wD} values.

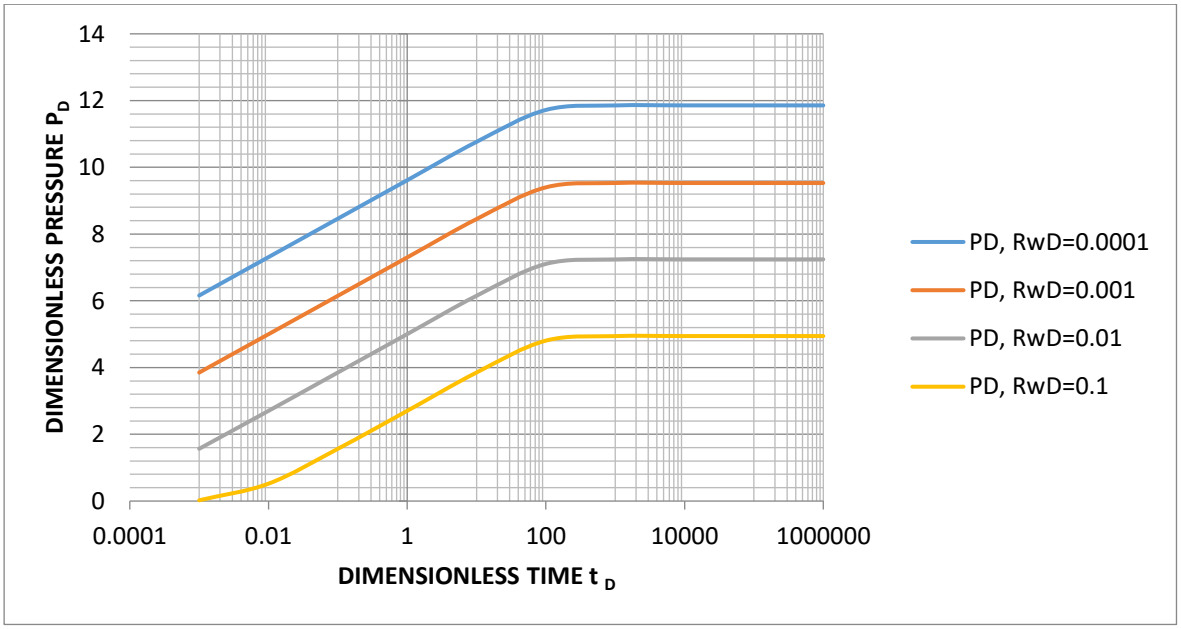

Figure 4: *Effect of changing dimensionless well radius r_{wD} on dimensionless pressure. α=2, L_D=1, k_x=100 md, k_y=150 md, k_z=200 md, k=144.2 md, c_D=1, dI_{w1}=20, dI_{w2}=28.3, dI_{w3}=20, S_{OW}= 0*

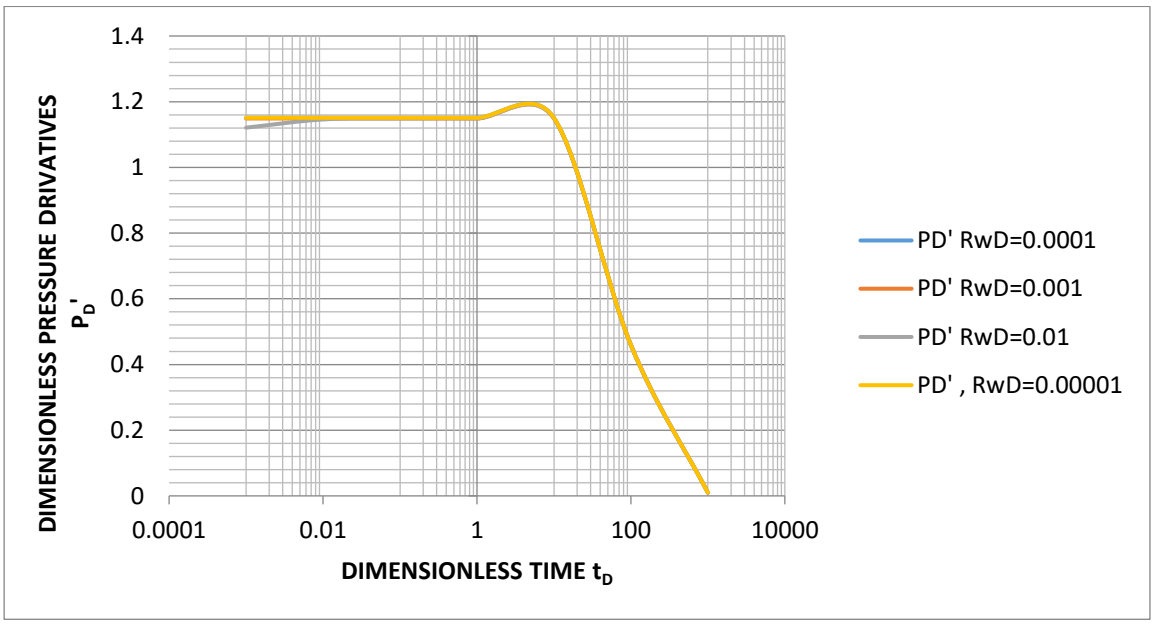

Figure 5: *Effect of changing dimensionless well radius on dimensionless pressure derivatives α=2, L_D=1, k_x=100 md, k_y=150 md, k_z=200 md, k=144.2 md, C_D=1, dI_{w1}=20, dI_{w2}=28.3, dI_{w3}=20, S_{OW}= 0*

Figure 6 predict the behavior of the well dimensionless pressure under different sizes of well length. It was observed that increase in dimensionless well length result to decrease in dimensionless pressures. Also the dimensionless pressure P_D values increase with increase in dimensionless time t_D from t_D =0.001 to 100 which means production will reduce with time and later maintain a stable value from t_D =1000 onward which is a steady state flow, as the flow encountered the effect of constant pressure boundary. Figure 7.0 shows that increase in dimensionless well length decreases P_D' values and does not have effect on breakthrough time as P_D' curve intersect t_D axes at t_D =1000 for all L_D values.

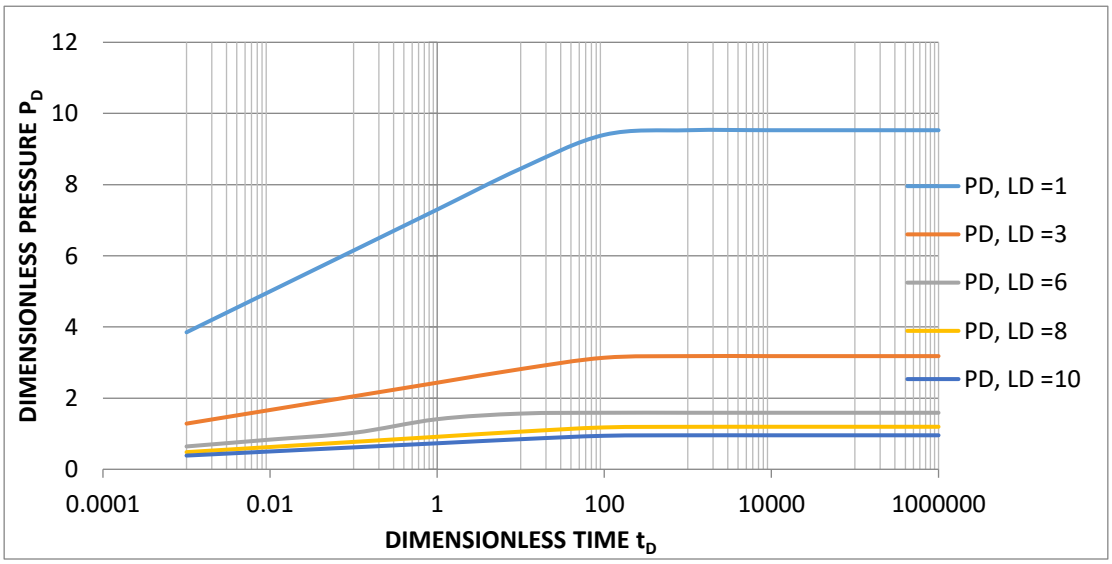

Figure 6: *Effect of changing dimensionless well Length L_D on dimensionless pressure α=2, r_{wD} =0.001, k_x=100 md, k_y=150 md, k_z=200 md, k=144.2 md, C_D=1, dI_{w1}=20, dI_{w2}=28.3, dI_{w3}=20, S_{OW}= 0*

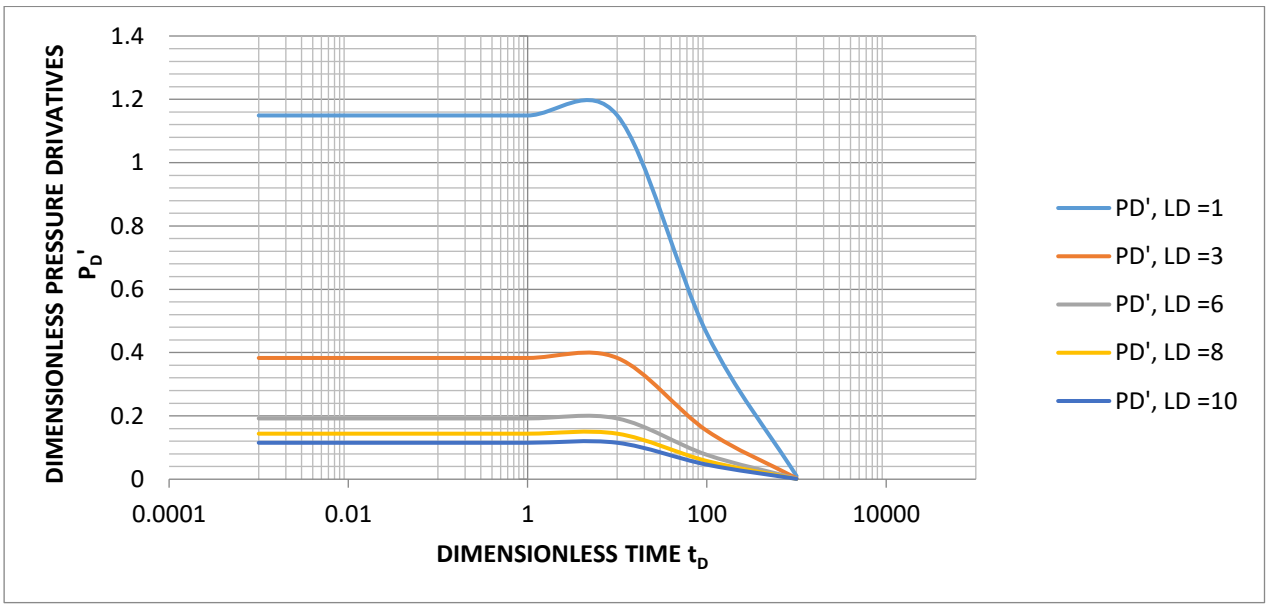

Figure 7: *Effect of changing dimensionless well Length L_D on dimensionless pressure derivatives P_D' α=2, r_{wD} =0.001, k_x=100 md, k_y =150 md, k_z=200 md, k=144.2 md, C_D=1, dI_{w1}=20, dI_{w2}=28.3, dI_{w3}=20, S_{OW}= 0*

Figure 8 show that increase in dimensionless wellbore storage decreases P_D values which would have a negative impact on production output. For the P_D' curve shown in figure 9 indicates that wellbore storage has no significant impact on P_D' as the curves for different C_D values merged to form a single curve. Also changing well bore storage has no effect on breakthrough time as the curve intersect t_D axes at t_D = 1000 dimensionless time for all C_D values.

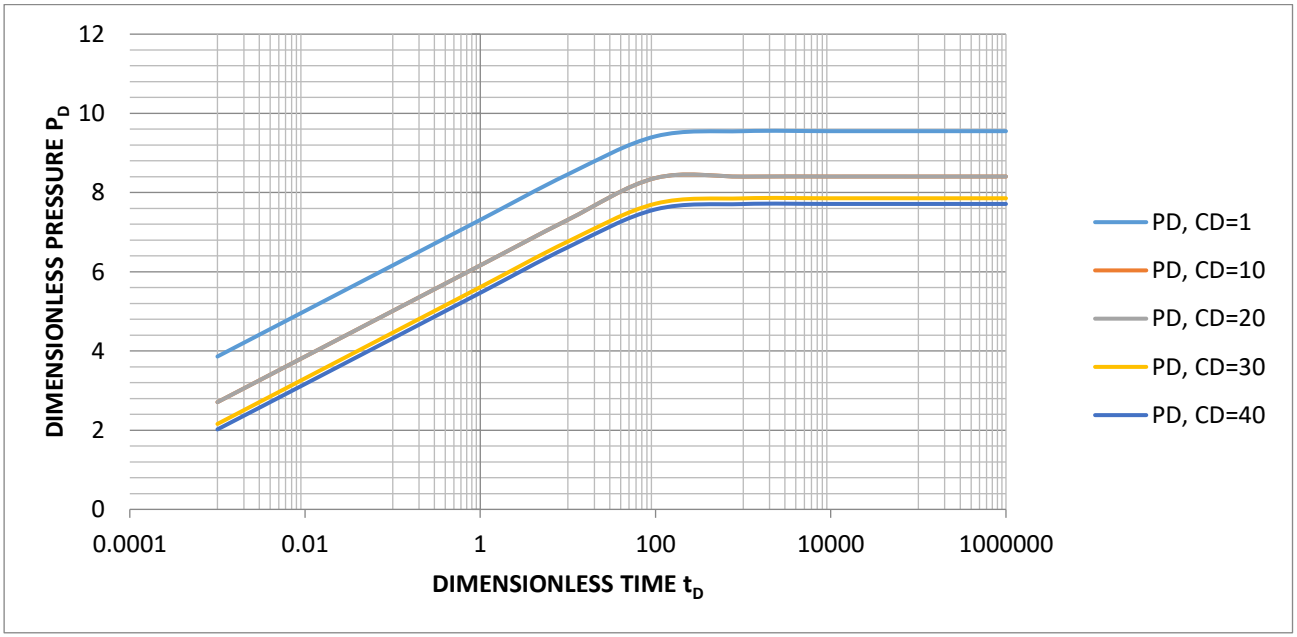

Figure 8: *Effect of changing dimensionless wellbore storage C_D on dimensionless pressure P_D α=2, r_{wD} =0.001, L_D=1, k_x=100 md, k_y =150 md, k_z=200 md, k=144.2 md, dI_{w1}=20, dI_{w2}=28.3, dI_{w3}=20, S_{OW}= 0*

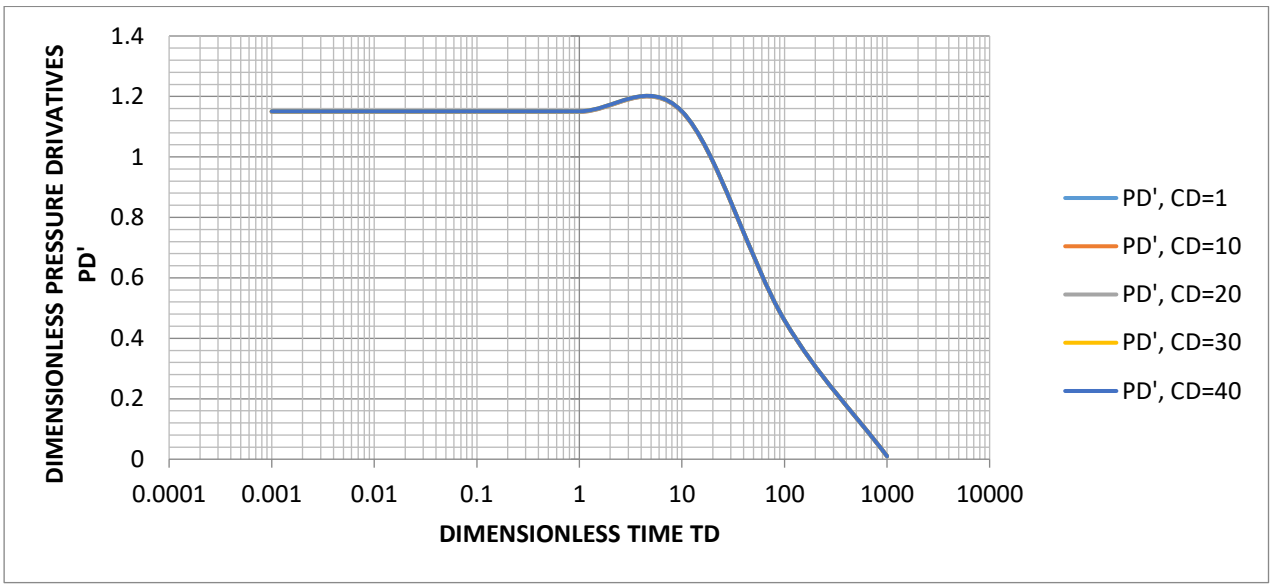

Figure 9: *Effect of changing dimensionless wellbore storage P_D on dimensionless pressure derivatives P'_D α=2, r_{wD} =0.001, L_D=1, k_x=100 md, k_y =150 md, k_z=200 md, k=144.2 md, dI_{w1}=20, dI_{w2}=28.3, dI_{w3}=20, S_{OW}= 0*

The result from Figure 10 depict that increase in image well distance did not affect P_D values for the infinite acting flow period and only clean oil is produced. As the flow enter transition period the P_D values begin to increase with increase in image well distance but at late time the P_D values become stable as the constant pressure boundary replenish the reservoir pressure. From Figure 11 it shows that P_D' curve has two point of intersection at t_D axes, t_D=100 and t_D=1000.This indicates that at short image well distance the breakthrough time is shorter (100) while longer image well distance has higher (1000) breakthrough time. Remember, image well distance is twice the distance of the object horizontal well from the boundary.

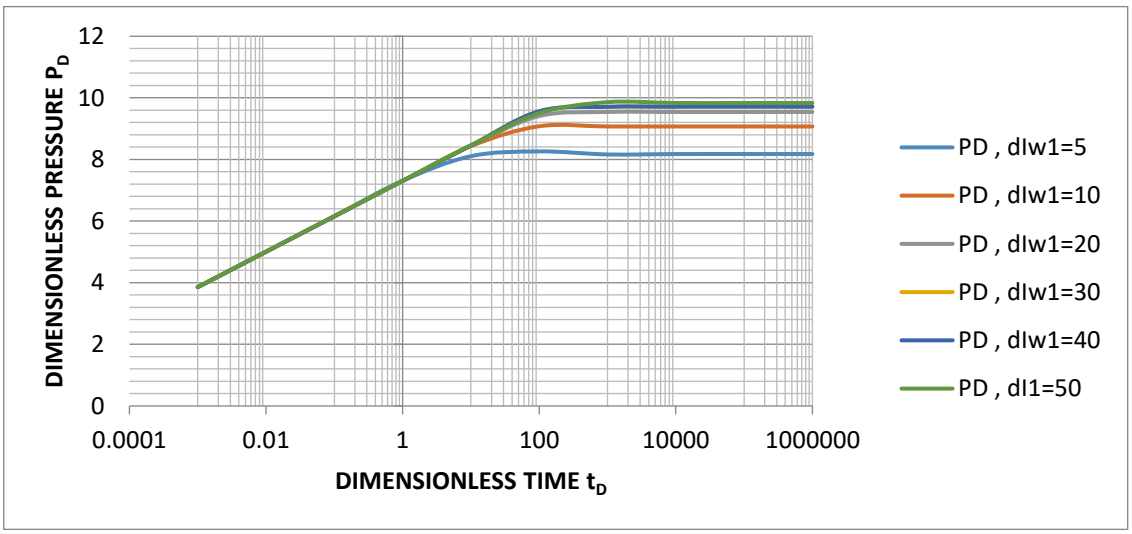

Figure 10: *Effect of changing dimensionless image well distance on dimensionless pressure P_D α=2, r_{wD} =0.001, L_D=1, C_D=1, k_x=100md, k_y =150 md, k_z=200 md, k=144.2 md, dI_{w2}=20.6, dI_{w2}=22.4, dI_{w2}=28.3, dI_{w2}=36.1, dI_{w2}=44.7 dI_{w2}=53.9, dI_{w3}=20, S_{OW}= 0*

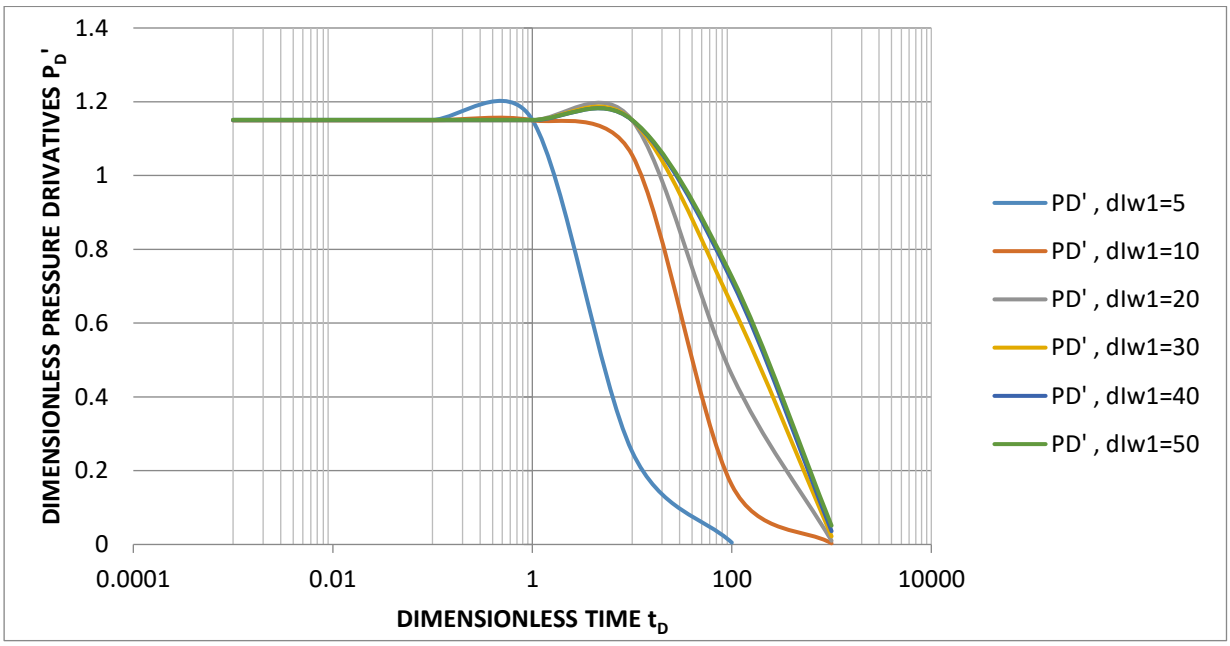

Figure 11: *Effect of changing dimensionless image well distance on dimensionless pressure derivatives P_D' α=2, r_{wD} =0.001, L_D=1, C_D=1, k_x=100md, k_y =150 md, k_z=200 md, k=144.2 md, dI_{w2}=20.6, dI_{w2}=22.4, dI_{w2}=28.3, dI_{w2}=36.1, dI_{w2}=44.7 dI_{w2}=53.9, dI_{w3}=20, S_{OW}= 0*

From Figure 12, it can be seen that negative skin factor of -2 and -1 give lower P_D values compare to values obtained with skin of zero, by implication the flow rate will be faster which can be due to well stimulation, re-perforation or improved well design. In the other hand positive skin factor of +1 and +2 yield P_D values greater than that of zero skin, this can result to decline in production output which is normally caused by formation damage. However the general trend of the curves is still similar to the zero skin, even with the lower or higher P_D values. Also skin does not have any significant effect on dimension less pressure derivatives.

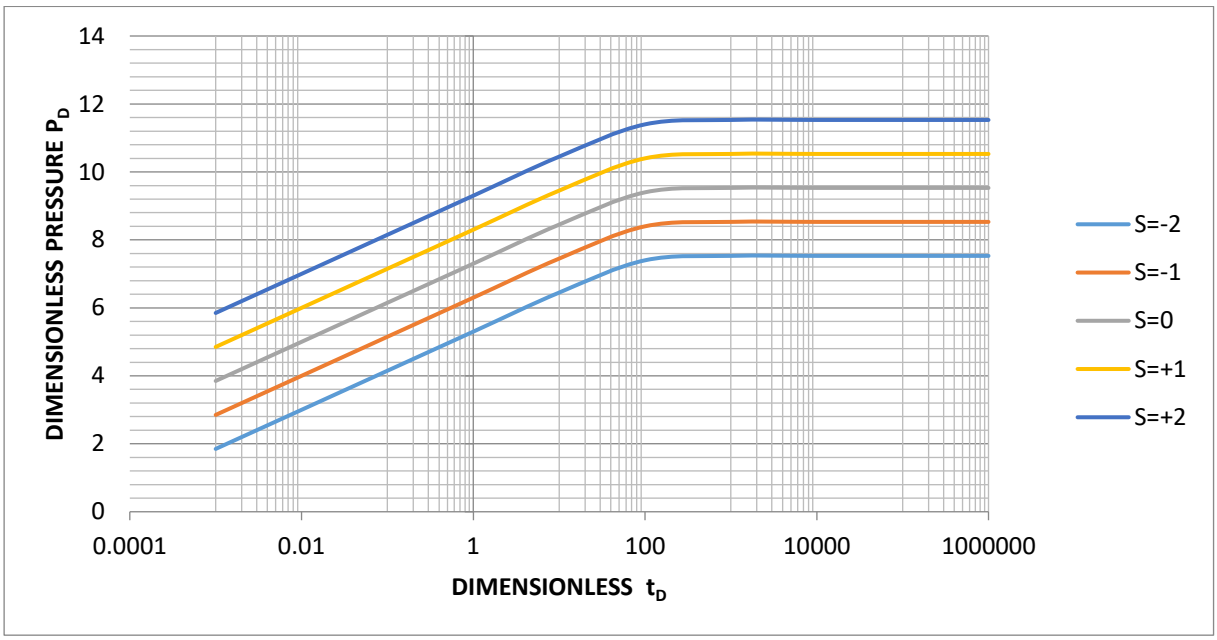

Figure 12: *Effect of changing dimensionless skin factor on dimensionless pressure. α=2, r_{wD} =0.001, L_D=1, C_D=1, k_x=100 md, k_y =150 md, k_z=200 md, k=144.2 md, dI_{w1}=20, dI_{w2}=28.3, dI_{w3}=20*

4. CONCLUSION

In this study the performance of a horizontal well subject to single edge and bottom water drive mechanism for anisotropic reservoirs was investigated analytically. The analytical models were tested to evaluate response to dimensionless pressure and derivative for five major parameters (dimensionless well radius r_{wD}, dimensionless well length L_D, dimensionless wellbore storage, dimensionless image well distance dI_{wD} and well skin factor).

After a thoughtful study, it was discovered that P_D values decreases for greater values of dimensionless wellbore radius r_{wD} and dimensionless well length L_D. But increase in dimensionless wellbore storage C_D decreases P_D values which would have a negative impact on production output. For dimensionless image well distance dI_w, the findings revealed that increase in image well distance did not affect P_D values for the infinite acting flow period, as the flow enter transition period the P_D values begin to increase with increase in image well distance but at late time the P_D values become stable as the flow felt the impact of constant pressure boundary. For skin factor, it was discovered that negative skin factor give lower P_D values compare to values obtained with skin of zero, which imply a better production output as flow rate will definitely improve, which can be due to well stimulation, re-perforation or improved well design. On the other hand, positive skin factor yield P_D values greater than that of zero skin. This can result to decline in production output.

Dimensionless well radius r_{wD}, Dimensionless wellbore storage C_D, and skin factor, S has no significant effect on dimensionless pressure derivative, P_D' while increase in dimensionless well length L_D decreases P_D' values but does not have effect on breakthrough time. The parameter with highest effect on P_D' and breakthrough time was found to be dimensionless image well distance, short image well distance shorten the time it takes water to breakthrough while extending it will also extend the breakthrough time.

It is therefore concluded for optimum performance of a horizontal well subjected to single edge and bottom water drive, selection has to favor slimmer well radius, shorter well length, negative or zero skin factors, minimum wellbore storage while keeping the well as far as feasible from the constant pressure boundaries.

CONFLICT OF INTEREST

No conflict of interest was declared by the authors.

REFERENCES

[1] Dake L.P. (1978). Fundamental of Reservoir Engineering. Elsvier ScientificPub.co 10:289-324.

[2] Dunsmuir J.H. and Stewart G. (1989). Analysis of Pressure and Production Data from the Westech field. *SPE Formation evaluation*, 4(2), 169-176.SPE-18118-PA.

[3] Etuwe, C. D. and Adewole, E. S. (2025). Effects of Horizontal Well Length on the Pressure of a Reservoir Subject to Double Edge and Bottom Water Drives. *Journal of Engineering for Development*, 17(1): 57 – 70.

[4] Nzomo T. K., Adewole S.E, Awuor K.O. and Oyoo D.O (2022). Performance of a horizontal well in a bounded anisotropic reservoir: Part I. Mathematical analysis. *Open Engineering*, 12: 17–28.

[5] Nzomo T. K., Adewole S.E., Awuor K.O. and Oyoo D.O. (2023). Performance of a horizontal well in a bounded anisotropic reservoir: Part II: Performance analysis of well length and reservoir geometry. *Open Engineering*, 13: 20-32.

[6] Ogunfeyimi and Adewole (2025). Productivity Performance of a Horizontal Well in an Oil Reservoir Bounded by Bottom Water and A Sealing Boundary Inclined At 45^o. *Journal of Engineering for Development*, 17(3): 99 – 114.

[7] Olokor, W. F. and Adewole E.S (2024). Pressure and Derivative Responses of a Horizontal Well in a Reservoir with Impermeable Boundaries Inclined at Right Angle. *Journal of Engineering for Development*, 16(2):110 – 129.

[8] Oloro J. O. and Adewole S.E. (2020). Performance and Behavior of a Horizontal Well in Reservoir Subject to Double-Edged Water Drive. *Nigerian Journal of Technology*, 39(2): 417-423.

[9] Oloro J.O. and Adewole E.S. (2019). Derivation of pressure distribution models for horizontal well using source function. *Journal of Applied Science Environmental Management,* 23(4), 575–583. https://www.ajol.info/index. php/jasem.

[10] Orene J.J. and Adewole E.S. (2020). Pressure distribution of horizontal well in a bounded reservoir with constant pressure top and bottom. *Niger J Technol.* 39(1):154–60.

[11] Quincy A. E. (2022). Pressure and Pressure Derivative of a Horizontal Well Subjected to a Single Edge and Bottom Water Drive. *FUPRE Journal of Scientific and Industrial Research*, 6 (1): 123-137.

NOMENCLATURE

$P_D = \frac{\mathrm{kh\Delta P}}{\mathrm{141.2q\mu B}}$ $t_D = \frac{\mathrm{0.000264\times 4kt}}{\mathrm{\phi\mu ctL2}}$

$r_{wd} = \frac{2rw}{L}$ $L_D = \frac{L}{2h}$ $\Delta P = P_i - P_{wf}$,

O_W = Object horizontal well, I_{w1} = dimensionless image well 1 distance from the object well

I_{w2} = Dimensionless image well 2 distance from the object well,

I_{w3} = Dimensionless image well 3 distance from the object well, K_x = Permeability in the Horizontal (X) Direction (md)

K_y = Permeability in Y-Direction (md) , K_z = Permeability in the Vertical (Z) Direction (md)

K = $=\sqrt[3]{k_x k_y k_z}$ Average Permeability (md) , Ei = Exponential integral function

L = Well length, ft , P_i = Initial reservoir pressure, psi, P_{wf} = Wellbore pressure, psi

C_D = Dimensionless wellbore storage, S = Skin , P_D = Dimensionless pressure

P_D' = Dimensionless pressure derivative , r_{wD} = Dimensionless wellbore radius

r_w = Wellbore radius, ft , t = Flow time, hours , t_D = Dimensionless time

B = Oil formation volume factor, bbl/stb , μ = Oil viscosity, md

Ct = Total compressibility, per psi , φ = Porosity, fraction Subscript ,

D = Dimensionless,

w = Wellbore